THE JOURNAL OF BIOLOGICAL CHEMISTRY VOL. 287, NO. 9, pp. 6735–6742, February 24, 2012


# The Molecular Chaperone gp96/GRP94 Interacts with Toll-like Receptors and Integrins via Its C-terminal Hydrophobic Domain*[S]

Received for publication, September 30, 2011, and in revised form, January 2, 2012 Published, JBC Papers in Press, January 5, 2012, DOI 10.1074/jbc.M111.309526

**Shuang Wu**[‡§], **Feng Hong**[§], **Daniel Gewirth**[¶], **Beichu Guo**[§], **Bei Liu**[§], **and Zihai Li**[‡§1]

*From the* [‡]*Department of Immunology, MC 1601, University of Connecticut School of Medicine, Farmington, Connecticut 06030-1601, the* [§]*Department of Microbiology & Immunology, Medical University of South Carolina (MUSC), Charleston, South Carolina 29425, and the* [¶]*Hauptman-Woodward Medical Research Institute, Buffalo, New York 14203*

**Background:** gp96 is a molecular chaperone that binds and chaperones TLRs and integrins. But the structural basis of such is unknown.
**Results:** Mutation of a C-terminal loop structure in gp96 abrogates its ability to bind and chaperone both receptors.
**Conclusion:** We have successfully mapped the client-binding domain of gp96.
**Significance:** This study shall facilitate the development of targeted gp96 inhibitors for treatment of inflammation.

**The structural basis for molecular chaperones to discern misfolded proteins has long been an enigma. As the endoplasmic reticulum paralogue of the cytosolic HSP90, gp96 (GRP94, HSP90b1) is an essential molecular chaperone for Toll-like receptors (TLRs) and integrins. However, little is known about its client-binding domain (CBD). Herein, we provide genetic and biochemical evidence to definitively demonstrate that a C-terminal loop structure, formed by residues 652–678, is the critical region of CBD for both TLRs and integrins. Deletion of this region affects neither the intrinsic ATPase activity nor the overall conformation of gp96. However, without it, the chaperoning function of gp96 collapses. We also find a critical Met pair (Met$^{658}$-Met$^{662}$) for the folding of integrins but not TLRs. Moreover, we find that the TLR binding to gp96 is also dependent on the C-terminal dimerization domain but not the N-terminal ATP-binding pocket of gp96. Our study has unveiled surprisingly the exquisite specificity of gp96 in substrate binding and suggests a manipulation of its CBD as an alternative strategy for targeted therapy of a variety of diseases.**

Known also as HSP90b1 (1), GRP94 (2), ERp99 (3), endoplasmin (4), and TRA-1 (5), gp96 (6) is the endoplasmic reticulum (ER)[2] paralogue of the cytosolic heat shock protein 90 (HSP90) (7). It has long been implicated in maintaining protein homeostasis in the secretory pathway by participating in the general folding mechanism of glycoproteins and facilitating the ER-associated degradation of misfolded proteins (8). A landmark mutagenesis study in a pre-B cell line *in vitro*, however, demonstrates that the clientele of gp96 is restricted to a relatively small number of proteins, including Toll-like receptors (TLRs) and integrins (9). This conclusion has been largely corroborated by extensive gene knock-out studies in mice (10–15). gp96 is among the highest conserved molecules along the phylogenic tree. For example, we have demonstrated that the *Drosophila* gp93, an ortholog of mammalian gp96, can fold both TLRs and integrins in gp96-null murine cells (16).

TLRs are important pattern recognition receptors for microbial products. There are 13 members of the TLR family in the mammalian system (17). TLR3, TLR7, TLR8, TLR9 and TLR13 are localized primarily in the endolysosomes, whereas the rest of TLRs are expressed on the cell surface. All TLRs are type I transmembrane receptors that form dimers in the ER for subsequent subcellular trafficking and function (18). The structure of TLRs includes a leucine-rich repeat (LRR)-containing ectodomain, a transmembrane domain, and a cytoplasmic tail that contains Toll/IL-1 receptor (TIR) domain. TLRs exploit their respective ectodomains to detect and bind to their specific microbial or endogenous ligands, followed by the initiation of signaling events via the TIR domain. Through multiple cytoplasmic signaling adaptors including MyD88, TIRAP, TRIF, and TRAM, TLR ligation can activate several signaling pathways including MAPK, IRF, and NF-$\kappa$B pathways and induce proinflammatory cytokine production (19). While TLRs serve as the first line of defense in innate immunity, they could also be implicated in pathological conditions such as endotoxic shock, autoimmunity, and inflammation-associated malignancy.

Similar to TLRs, integrins are type I transmembrane receptor dimers formed by $\alpha$ and $\beta$ subunits. There are 18 $\alpha$ subunits and 8 $\beta$ subunits, which heterodimerize to form 24 distinct integrin members (20). Integrins collectively play multi-faceted functions in cell migration, adhesion, survival, and apoptosis as well as in cell polarization and chemotaxis (20–22). Although TLRs and integrins do not share apparent structural homology, the proper folding and subcellular distribution of a majority of TLRs and integrins is unexpectedly and absolutely dependent on gp96 (9, 10).

* This work was supported, in whole or in part, by National Institutes of Health Grants AI070603, AI077283, and HL100556 (to Z. L.), and by the Flow Cytometry Shared Resource, Hollings Cancer Center, Medical University of South Carolina (P30 CA138313).
[S] This article contains supplemental Table S1 and Figs. S1 and S2.
[1] To whom correspondence should be addressed: Hollings Cancer Center, Department of Microbiology & Immunology, Medical University of South Carolina (MUSC), Charleston, SC 29425. Tel.: 843-792-1034; E-mail: zihai@musc.edu.
[2] The abbreviations used are: ER, endoplasmic reticulum; TLR, Toll-like receptor; CBD, client-binding domain; HSP, heat shock protein.

Both gp96 and HSP90 contain a N-terminal ATP-binding pocket with intrinsic ATPase activity, followed by the middle charged domain and the C-terminal homodimerization domain (23, 24). However, the client-binding domain of both molecules and the respective chaperoning mechanism still await elucidation. The crystal structure of the C-terminal dimerization domain of the *Escherichia coli* HSP90 homolog, HtpG, showed that helix 2 of this domain (residues 548–557) formed a potential client binding surface (25). Subsequently, a mutagenesis study of residues along the same helix in mammalian HSP90 abolished its binding to the glucocorticoid receptor (26). Despite these intriguing early studies, however, it remains unclear if this region is important for chaperoning other client proteins and how client protein specificity is determined.

A corresponding C-terminal loop structure, formed by residues 652–678, is present in gp96 (24), raising an intriguing possibility of such a loop as a part of the client-binding domain (CBD) of gp96. We have addressed this hypothesis both genetically and biochemically. We found indeed that residues 652–678 of gp96 are critical for client binding and for chaperoning both TLRs and integrins, but not for ATPase activity, C-terminal dimerization or overall stabilization of the protein. We have also identified the critical residues in this region that are selectively required for folding integrins but not TLRs.

## EXPERIMENTAL PROCEDURES

*Constructs and Site-directed Mutagenesis*—Wild type murine gp96 cDNA in a pGEM-T Easy vector (Promega) was used as templates for all PCR. Primers for gp96 mutants were listed in supplemental Table S1. ΔCBD, NTD+CBD, NTDΔCBD, CTD+CBD, CTDΔCBD were constructed by fusion PCR utilizing respective primers with HF Pfu (invitrogen). AA1, AA2 as well as all gp96 Met mutants were generated using the QuikChange II XL Site-directed Mutagenesis kit (Stratagene). All constructs were subcloned into MigR1 retroviral vector for retrovirus production. MigR1-TLR4HA and MigR1-TLR9HA were described in Ref. 10.

*Cloning and Purification of Recombinant Protein*—The coding sequence of mouse gp96 73–754 ΔCBD (652–678) was amplified by PCR and cloned into the NdeI/BamHI sites of pET15b. BL21 Star (DE3) cells bearing this plasmid were grown at 37 °C in LB media under Ampicillin selection to an $A_{600}$ of 1, and protein production was induced by the addition of IPTG to a final concentration of 0.5 mM. gp96 was purified according to the published method (24), concentrated to 30 mg/ml and stored frozen at −80 °C. His-tagged canine gp96 73–754 and *E. coli* HtpG were purified in an identical manner.

*Analytical Gel Filtration Chromatography*—6–8 mg of purified gp96 ΔCBD or gp96 73–754 were diluted to 1 ml with 10 mM Tris, pH 7.6, 150 mM NaCl, 1 mM DTT, and applied to a Superdex S200 16/60 column equilibrated in the same buffer. The elution was monitored by absorbance at 280 nm.

*ATPase Measurements*—ATP hydrolysis measurements were carried out using the PiPer assay kit (Stratagene), which measures the amount of free phosphate liberated in a hydrolysis reaction. gp96 73–754, gp96 ΔCBD, and HtpG were buffer exchanged into assay buffer (40 mM Hepes, pH 7.4, 150 mM KCl, 5 mM $MgCl_2$) and diluted to 11 μM in assay buffer prior to use. The hydrolysis experiment was carried out in 96-well fluorescent assay plates. Each well contained a mixture of 5 μl of ATP (0–16 mM, in assay buffer), 45 μl of protein, and 50 μl of PiPer reagent (100 μM Amplex Red, 4 units/ml maltose phosphorylase, 0.4 mM maltose, 2 units/ml glucose oxidase, 0.4 units/ml horseradish peroxidase, 100 mM Tris, pH 7.5). The final concentration of protein in each well was 5 μM, and the final ATP concentration varied from 0–800 μM. Reactions were carried out in duplicate. Plates were incubated at 37 °C, and the reaction was stopped after 100 min by burying the plastic wrapped plate in ice. Fluorescence was measured at 544 nm/590 nm (excitation/emission) on a SpectraMax Gemini XS plate reader (Molecular Devices) with 30 readings per well. Data were corrected by first subtracting the reading where the ATP concentration was 0. This was followed by subtracting the average of the readings carried out in the absence of protein for each ATP concentration tested. Kinetic parameters were determined using the program Prism according to the one site binding hyperbola equation $Y = V_{max} \times X/(K_d + X)$.

*Cell Lines*—All gp96 mutant-transduced PreB cell lines were generated from parental gp96-null E4.126 PreB cell line, which was a kind gift from B. Seed (Harvard). Phoenix Eco (PE) packaging cell line from ATCC was used for retrovirus production. All culture conditions have been previously described in Ref. 16.

*Antibodies and Peptides*—gp96 N terminus antibody 9G10 and gp96 C terminus antibody SPA851 were purchased from Enzo Life Sciences and detected both endogenous and overexpressed proteins. β-Actin antibody, HA1.1, and Flag antibody bioM2 were from Sigma. Biotin-conjugated anti-mouse CD11a (Clone: M174), CD49d (Clone: R1–2), CD18 (Clone: M18/2), TLR2 (Clone: 6C2), and TLR4 (Clone: MTS510) antibodies used for flow cytometry were purchased from eBioscience and they detected endogenous proteins. TAT-CBD peptide contains TAT sequence (YGRKKRRQRRR) and amino acids 652–678 of gp96. It was synthesized by NEO group to more than 98% purity as verified by HPLC and mass spectrometry.

*Retrovirus Production and Transduction*—Various MigR1-gp96 mutants were transfected into PE cell line using Lipofectamine 2000 (Invitrogen). Six hours after transfection, medium was replaced by pre-warmed fresh culture medium. Virus-containing medium was collected at 24 h and 48 h after transfection. To facilitate the virus adhesion, spin transduction was performed at 1800 × *g* for 1.5 h at 32 °C in the presence of 8 μg/ml hexadimethrine bromide (Sigma).

*Blasticidin Selection*—A blasticidin resistant gene was bicistronically expressed downstream of the target gene in the MigR1 vector. All transduced PreB cells were selected for a week in RPMI culture medium containing 0.5 μg/ml blasticidin to ensure a relatively homogenous population and comparable expression level between all mutants.

*Flow Cytometry*—All staining protocol, flow cytometry instrumentation as well as data analysis were performed as described without significant modifications (12, 16). For cell surface staining, single cell suspension of live cells was obtained and washed in FACS buffer twice. FcR blocking with or without serum blocking was performed depending on individual primary antibody used for staining. Primary and secondary anti-

bodies staining were performed stepwise, with FACS buffer washing in between. Propidium iodide (PI) was added right before FACS instrumentation to gate out dead cells. For intracellular staining, cells were fixed in 4% paraformaldehyde at room temperature, then permeabilized with ice-cold methanol at −20 °C. Blocking and staining procedures were similar to surface staining, except all steps were done at room temperature. Stained cells were acquired on a FACS Calibur (BD Biosciences) and analyzed using the FlowJo software (Tree Star).

*NF-κB GFP Reporter Assay*—As described in Ref. 9, all cells derived from E4.126 parental cell line contain the NF-κB-driven GFP reporter. Cells were stimulated with Pam3CSK4 (10 μg/ml), LPS (10 μg/ml), CpG ODN1826 (5 μM), PMA (100 ng/ml), and ionomycin (2 μg/ml) for 16–18 h before FACS instrumentation.

*SDS-PAGE, Western Blot, and co-IP*—Essentially all procedures were performed as described in Ref. 16, without significant changes.

*Statistical Analysis*—Error bars represent the standard error of the arithmetic mean (S.E.). Student's *t* test was used for statistical analysis. Values of $p < 0.05$ (*) were considered to represent statistically significant differences.

## RESULTS

*Deletion of Amino Acid 652–678 Abolishes the Function of gp96*—The 27 amino acid C-terminal loop structure of gp96 includes several highly hydrophobic residues including Met, Trp, and Tyr. Yet, this structure appears to be flexible and pointing out to the solvent, providing a potential site for client binding (24) (Fig. 1*A*). To test this possibility, we made a deletion mutant of gp96 without this region, named gp96 ΔCBD (Fig. 1*A*). The 652–678 region is hereafter referred to as the putative CBD. To examine the impact of this deletion on the overall conformation of the protein, we expressed the protein recombinantly. We found that deletion of the CBD does not affect the ability of gp96 to dimerize as revealed by size exclusion chromatography (Fig. 1*B*). Moreover, the ATPase activity of ΔCBD is completely preserved (Fig. 1*C*). To determine the functional impact of ΔCBD on gp96 in mammalian cells, we took an advantage of a gp96 mutant PreB cell line, E4.126, which lacks gp96 (9). We were able to express both wild type (WT) and ΔCBD in the mutant PreB cell line (Fig. 1*D*). More importantly, by immunoprecipitation (IP), we found that the mutant remains capable of binding to a recently discovered gp96 co-chaperone CNPY3 (Fig. 1*E*). CNPY3 binding site has been mapped to the N terminus of gp96 (11). These data indicate that deletion of 652–678 does not affect the overall conformation of gp96.

We next examined the chaperoning function of gp96 based on the cell surface expression level of its client proteins. As expected from the previous studies (9–12, 27), WT gp96 can restore the cell surface expression of all gp96 clients examined including integrin αL, β2, and α4, TLR2 and TLR4 (Fig. 1*F*). However, ΔCBD mutant was unable to rescue the expression of any of these clients. In addition, consistent with the functional restoration of TLRs, WT gp96-transduced cells responded well to Pam3CSK4 (a TLR2 ligand), LPS (a TLR4 ligand) and CpG oligonucleotide (a TLR9 ligand), measured by a NF-κB-GFP reporter assay (Fig. 1*G*). However, ΔCBD transduced cells were unable to activate NF-κB in response to any of the TLR ligands tested despite a similar reporter expression level as demonstrated by PMA/ionomycin stimulation. We conclude thus that ΔCBD is a novel functional null gp96 mutant despite its intact ability to dimerize, hydrolyze ATP, and to interact with its co-chaperone.

*Essential Role of GWXGNMER Motif within the CBD in the Function of gp96*—Comparison of gp96 with *Drosophila* gp93 (16) demonstrates a high sequence homology within the putative CBD region, particularly in the first half of sequence where a conserved GW*X*GNMER motif is present (Fig. 2*A*). We next performed an Ala-scanning mutagenesis and generated two mutants: AA1 with all the conserved residues in the first half of CBD mutated to Ala and AA2 with Ala substitution of all the conserved residues in the second half of CBD. Retroviral mediated transduction was performed to introduce these mutants into gp96-null PreB cells. Surface expression of integrins and TLRs on the transduced cells were examined by flow cytometry. Whereas both AA1 and AA2 gp96 mutants could be expressed to a similar level to WT gp96, only WT but not AA1 was able to rescue the cell surface expression of clients (Fig. 2*B*). The client expression was reduced but not abrogated completely in AA2-expressing cells. Thus, the most severe defect is ΔCBD mutant, followed by AA1 mutant and AA2 mutant. As expected, AA1 failed to functionally restore TLR responsiveness of gp96-null cells (Fig. 2*C*). These data demonstrated the essential roles of GWXGNMER motif in the function of gp96.

*Critical Roles of Met$^{658}$ and Met$^{662}$ for Chaperoning Integrins but Not TLRs*—A pair of Met residues in HSP90 is essential for chaperoning the glucocorticoid receptor (26). In gp96, Met$^{658}$ and Met$^{662}$ of the putative CBD form a similar pair that, together with the neighboring hydrophobic resides (Tyr$^{575}$, Tyr$^{652}$, Trp$^{654}$, Tyr$^{677}$, Tyr$^{678}$) form a hydrophobic patch on the bottom of the "V" shaped structure of the gp96 dimer (Fig. 1*A*). To define the role of this Met pair, we mutated both Met (M2A) as well as each of the two Met (M658A, M662A) separately into Ala using site-directed mutagenesis. Unexpectedly, the M2A mutant was able to fully restore the expression of TLR2 and TLR4, but was defective in chaperoning integrins (Fig. 3*A*, $p < 0.01$). While the phenotype of the single M658A or M662A mutants resembles that of M2A, the M2A mutant suffered the greatest defect in chaperoning integrins. Quantification of client expression after normalization for gp96 expression levels confirmed the substrate specificity of the M2A mutants (Fig. 3*B*). None of the Met mutants had any problems in rescuing gp96-null cells for TLR responsiveness (supplemental Fig. S1, *A* and *B*). In fact, the TLR2-chaperoning function of M658A is even better than that of wild type gp96, although its ability to restore cell surface expression of αL, β2, and α4 integrins is significantly impaired. The M658/M662 region of the gp96 CBD thus appears to confer client specificity to the chaperone.

*Impaired Binding of CBD Mutants to TLRs*—We next examined if mutation of CBD region impairs the interaction between gp96 and its clients. To do this, we co-expressed C-terminal HA-tagged TLR9 (TLR9HA) with gp96 in PreB cells (Fig. 4*A*) and performed a co-immunoprecipitation (co-IP) assay. As expected, we could readily co-IP TLR9HA with WT gp96. The

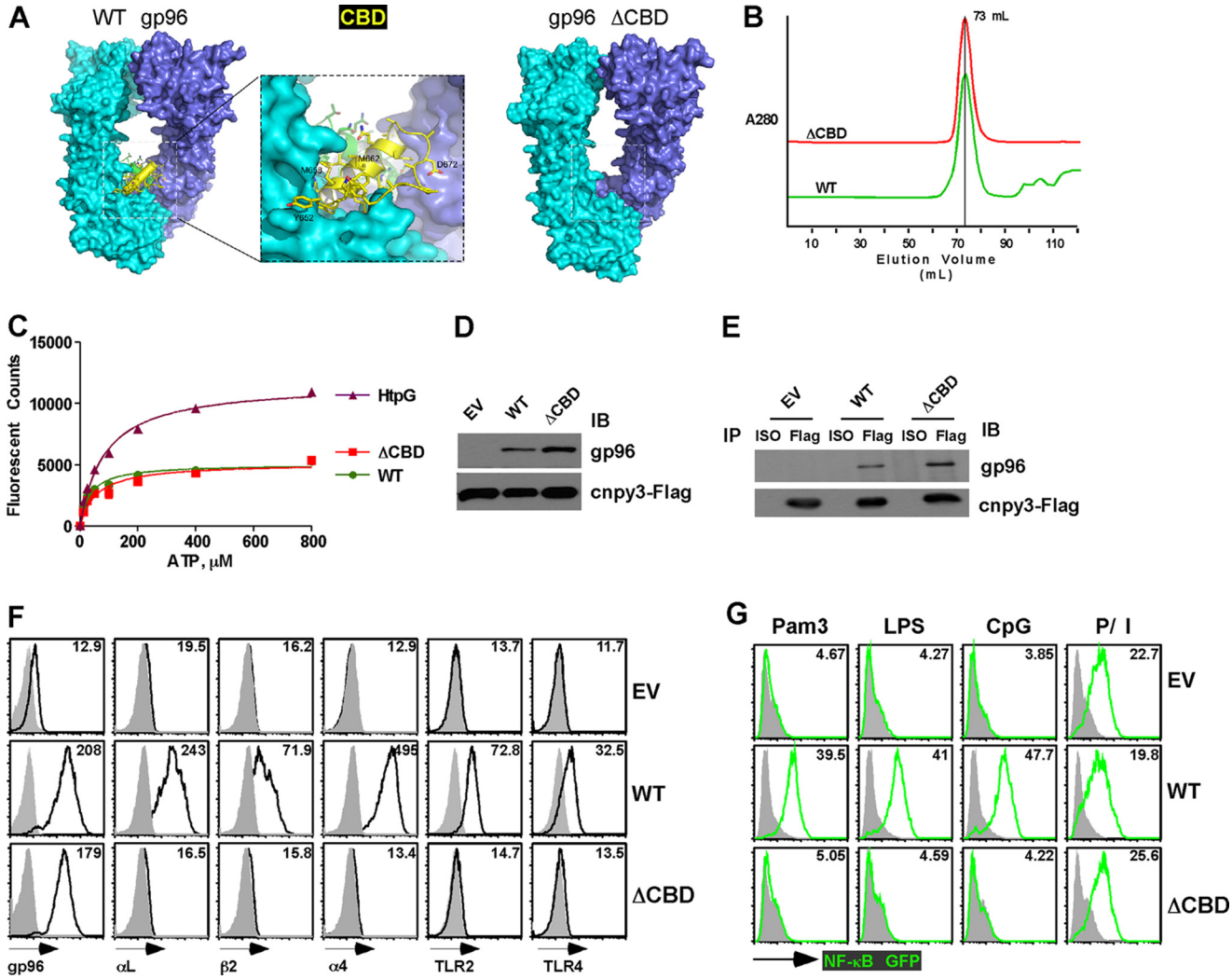


FIGURE 1. **A deletion mutant of the C-terminal loop structure abolishes the chaperone function of gp96.** *A*, left, a wild type gp96 homodimer structure is shown with the proposed client binding domain of gp96 (652–678) highlighted in *yellow*. The blow-up shows the CBD as a helix-loop structure in the C-terminal of gp96. *Right*, ΔCBD mutant is modeled to preserve the overall structure of gp96. *B*, ΔCBD and WT gp96 exhibit identical behavior on gel filtration chromatography. 5–8 mg of purified protein was injected for each run, and the elution was monitored by absorbance at 280 nm. The peak at 73 ml contains gp96 dimer (~200 kDa). *C*, ΔCBD and WT gp96 exhibit identical ATP hydrolysis rates. ATP hydrolysis was measured using the PiPer assay system, which monitors free phosphate. The protein concentration in the reaction was 5 μM, and was carried out at 37 °C for 100 min. *D*, ΔCBD mutant can be stably expressed in the gp96-null E4.126 cells. gp96, ΔCBD mutant and CNPY3-Flag were introduced into E4.126 cells by MigR retrovirus. Expression level was determined by SDS-PAGE. Empty virus (*EV*) was used as a control. *E*, both gp96 and ΔCBD mutant are able to interact with CNPY3. CNPY3-Flag was immunoprecipitated followed by immunoblot (*IB*) for gp96 or CNPY3. *F*, intracellular staining of gp96 and surface expression of integrins and TLRs (*solid line histogram*) in gp96-null pre-B cells transduced with WT or ΔCBD mutant. *Gray histograms* are isotype control antibody stain. Number represents mean fluorescence intensity (*MFI*) of TLRs or integrins. *G*, NFκB-GFP reporter activation (*green histogram*) of cells in E after overnight (16–18 h) stimulation with Pam3CSK4 (10 μg/ml), LPS (10 μg/ml), CpG (5 μM), or P/I, which contains PMA (100 ng/ml) and ionomycin (2 μg/ml). *Gray histograms* are GFP profile of unstimulated cells.

AA2 mutant, in which the conserved residues in the second half of the gp96 CBD is mutated to Ala, retains some binding capacity to TLR9HA, while the ΔCBD and AA1 mutants completely lost their ability to interact with TLR9HA (Fig. 4*B*). In agreement with the functional data presented above, the M2A, M658A, and M662A mutants could be stably expressed (Fig. 4*C*), and were able to interact with TLR9HA (Fig. 4*D*). Consistent with the ability of M2A mutant to be fully functional in folding TLRs, we found that the M2A mutant remains capable of binding to CNPY3 (supplemental Fig. S2).

*Soluble CBD Peptide Inhibits gp96-Integrin Interaction*—We next examined the possibility of direct binding between gp96 and integrin. Because the Met pair is located within the CBD, we hypothesized that the defect of chaperoning integrins by M2A mutant, as well as single Met mutants, is due to a problem in binding to integrins. To examine this hypothesis, we co-expressed αL-HA with the gp96 M2A mutant in HEK293 cells by transient transfection. As shown in Fig. 5*A*, αL-HA was equally expressed in the EV, WT and M2A mutants. However, when we used co-IP to examine the interaction between αL-HA and gp96, we found that the M2A mutant did not interact with αL as strongly as WT gp96 (Fig. 5*A*).

To further characterize the interaction between integrins and gp96, we performed a competition experiment with a synthetic peptide that corresponds to CBD. We incubated cells with increasing concentration of a cell-permeable TAT-CBD peptide 24 h prior to cell lysis. We then performed IP analysis to examine the interaction between gp96 and αL-HA. We found

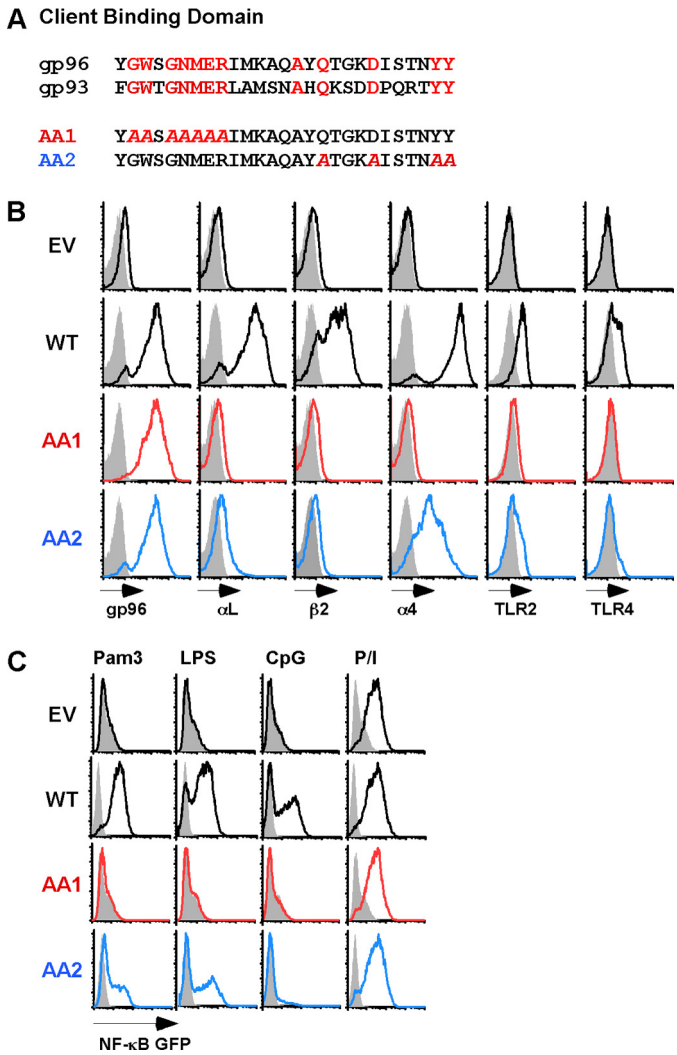


FIGURE 2. **Fine mapping of critical residues in gp96 (652–678) for chaperoning TLRs and integrins.** *A*, alignment of the sequence within the CBD between murine gp96 and *Drosophila* gp93. Residues highlighted in red are conserved between gp96 and gp93. Residues in *italic* are ones mutated into Ala. *B*, intracellular staining of gp96 and surface expression of integrins, TLR2 and TLR4 in gp96-null pre-B cells transduced with AA1 (*red*) or AA2 (*blue*) mutants (*Gray*: isotype; *solid line*: client staining). *C*, NFκB-GFP activity (*open histogram*) in *B* after overnight (16–18 h) stimulation with various TLR ligands. *Gray histogram* refers to GFP of unstimulated cells.

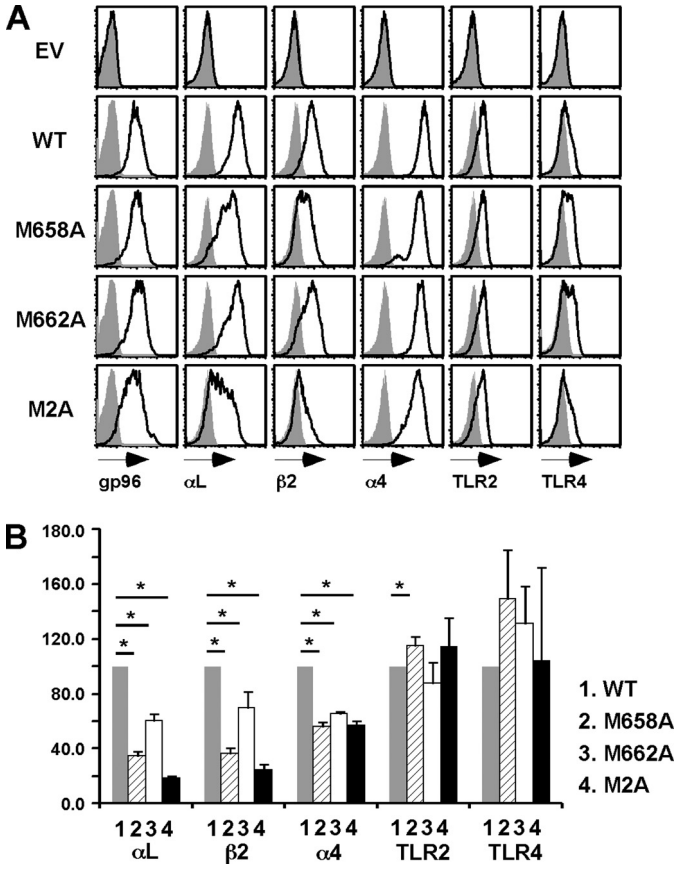


FIGURE 3. **Critical roles of Met$^{658}$ and Met$^{662}$ within the CBD for chaperoning integrins but not TLRs.** *A*, intracellular staining of gp96 and surface expression of integrins and TLRs in gp96-null pre-B cells transduced with different CBD mutants (*gray*: isotype; *solid line*: client stain). *B*, quantification of the mean fluorescence intensity (*MFI*) of client expression from three independent experiments. Error bars represent S.E. *, $p < 0.05$.

that TAT-CBD dose-dependently inhibited the ability of gp96 to interact with αL-HA (Fig. 5).

*Importance of the Dimerization Domain but Not the ATP-binding Pocket in Addition to the 652–660 Region of gp96 for Client Interaction*—We so far demonstrated that the CBD is necessary for gp96 to bind and functionally mature client proteins. We next asked if the putative CBD is also sufficient for interaction with clients. To test this possibility, we made a series of both N-terminal and C-terminal truncation mutants of gp96 with and without the CBD. These mutants contain both the canonical signal peptide for ER insertion and the KDEL ER retention signal to ensure the proper ER targeting (Fig. 6*A*). We introduced these truncation mutants to gp96-null PreB cells, along with TLR9HA (Fig. 6*B*). Consistent with the importance of the CBD, in the absence of it, neither the N-terminal domain (NTDΔCBD) nor the C-terminal domain of gp96 (CTDΔCBD) was able to efficiently co-IP with TLR9HA (Fig. 6, *C* and *D*). Importantly, we found that binding to TLR9 by gp96 is dependent on both the CBD and the CTD (Fig. 6*D*). The NTD+CBD mutant was unable to interact with TLR9 (Fig. 6*C*). We conclude that client interaction is dependent on both CBD and the C-terminal dimerization domain of gp96.

## DISCUSSION

Molecular chaperones have an intrinsic ability to discern the unfolded or misfolded conformation of a protein substrate from its folded mature state. The broad substrate specificity of most chaperones suggests that they do not contain just a single specific substrate-binding surface. The ER luminal protein gp96, on the other hand, appears to be a chaperone with selective substrate specificity, making it possible to define a specific client-binding region on gp96. In this study, using biochemical and cell biological approaches, we have demonstrated that a C-terminal loop structure, formed by residues 652–678, is a critical region for gp96 to bind to TLRs and integrins. This region is not required for the overall structural integrity of gp96, since we have shown that deletion of this domain does not alter the hydrodynamic, dimerization, co-chaperone binding, or ATP hydrolysis properties of the molecule. Rather, this region appears to be the locus of a physical interaction with

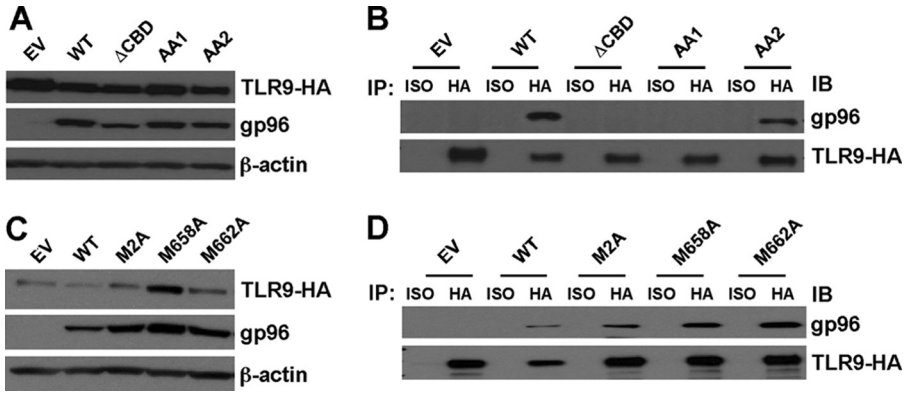


FIGURE 4. **Impaired interaction between gp96 CBD mutants and clients.** *A*, immunoblot of various gp96 CBD mutants and TLR9-HA in transduced gp96-null E4.126 cells. *B*, IP of TLR9-HA in multiple mutant cells followed by immunoblot for gp96 or TLR9HA. *C*, expression of various gp96 Met mutants as well as TLR9-HA in gp96-null E4.126 cells. *D*, WT gp96 or various mutants were transduced into gp96-null E4.126 cells. IP was performed as in *B*.

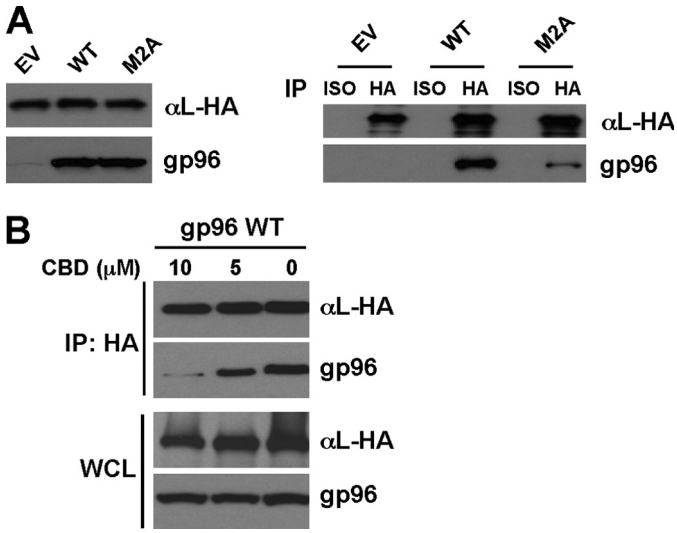


FIGURE 5. **Interaction between gp96 and αL-integrin can be inhibited by a cell-permeable CBD peptide.** *A*, left, expression of WT and M2A mutant and αL-HA in HEK293 cells after transient transfection. *Right*, IP of αL-HA followed by immunoblot for gp96 or αL-HA. *B*, TAT-CBD peptides reduced interaction of gp96 and αL-HA. HEK-293T cells were co-transfected with mouse gp96 (WT or M2A mutant) and αL-HA. TAT-CBD peptides were added into medium 24 h post-transfection, and incubated for additional 24 h. Cells were then harvested. αL-HA precipitates were resolved and immunoblotted for mouse gp96. Whole cell lysate (*WCL*) were also blotted for respective proteins as a control.

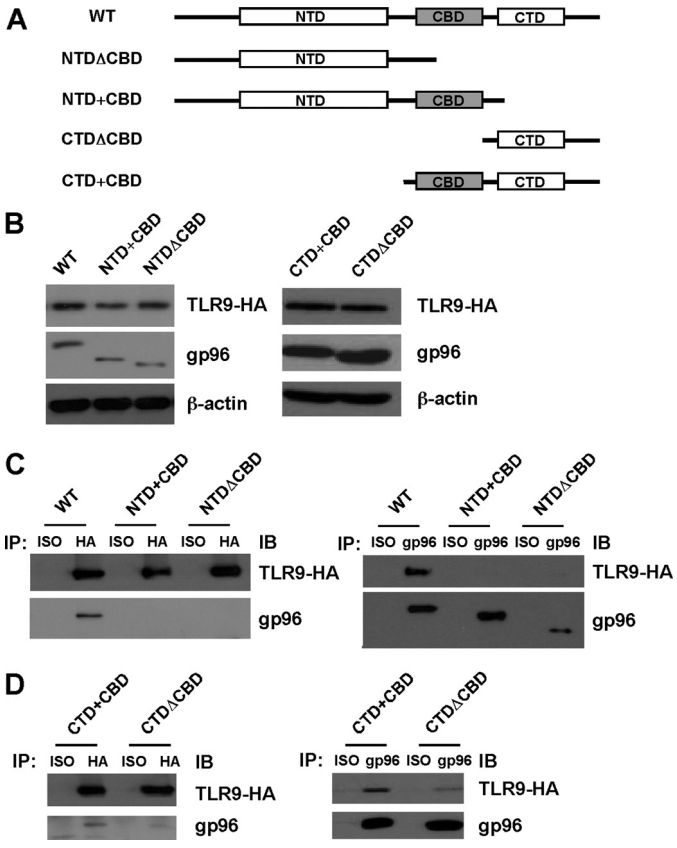


FIGURE 6. **TLR9 binding to gp96 is dependent on both CBD and the C-terminal dimerization domain of gp96.** *A*, illustration of different gp96 N-terminal or C-terminal truncation mutants. *B*, immunoblot analysis of different gp96 truncation mutants as well as TLR9-HA. *C*, interaction between TLR9-HA and NTD + CBD or NTDΔCBD truncation mutants. gp96 or TLR9HA was immunoprecipitated followed by IB with indicated antibodies. *D*, interaction between TLR9-HA and CTD + CBD or CTDΔCBD truncation mutants. Co-IP was performed as in *C*.

both integrins and TLRs. This conclusion is further strengthened by the finding that within the 652–678 region of gp96 two residues control substrate specificity: $Met^{658}$ and $Met^{662}$ are critical for gp96 to bind integrins but not to TLRs.

The crystal structure of gp96 resembles a "twisted V" shaped structure that is dimerized via its paired C-terminal domains. This resembles the structure of the cytosolic counterpart of gp96 known as HSP90. Although the broad client repertoire of HSP90 has been defined, the client-binding domain of HSP90 remains unclear (28). Several regions of HSP90 have been implicated in protein-protein interaction, including a negatively charged region in the N terminus (221–290), another negatively charged region in the C terminus (530–581) and the middle region with a leucine zipper structure (392–419) (29). Different regions including 381–441 and 601–677 of chicken HSP90 have been mapped to interact with progesterone receptor (PR) (30). The folding of MyoD1, a basic helix-loop-helix (bHLH) protein, appears to depend on the last 194 amino acids of the C-terminal mouse HSP90 (31). These observations suggest that HSP90 possesses disparate binding sites for its diverse clientele.

HSP90 belongs to GHKL superfamily whose members, include GyrB and MutL (23). After comparing the crystal structure of the middle domain of HSP90 to other GHKL members, it was brought to attention of a conserved hydrophobic patch

around Trp-300 and an amphipathic loop (327–340) extending out from the middle domain of HSP90 (32). Deletion of a conserved 13 amino acid sequence between HSP90a and HSP90b (327–340) abolished the interaction between HSP90 and AKT in murine 3T3 and human 293T cells (33). This results in a proposal of a "molecular clamp" model similar to other GHKL family member, in that HSP90 binds to client between the M-domain of two monomers, and it releases the client in the more tensed structure induced by ATP hydrolysis (32). This is supported by a HSP90-Cdk4-Cdc37 trimolecular model (34). In this model, the two kinase lobes of Cdk4 bind to the M-domain and N-domain respectively, spanning across the N-M region. The larger lobe of Cdk4 interacts with M-domain via the amphipathic loop (35). As the N-M domain undergo further twisting, the proposed loop extends outwards of the HSP90 dimer, and pushes Cdk4 to the outside of the HSP90 clamp.

Recently, it has been indicated that a helix structure of the C-terminal dimerization domain could be a substrate-binding site of HSP90. The crystal structure of the dimerization domain of *E. coli* HtpG observed that Helix 2 (544–565) resides in the jaw of HtpG dimer, loops out toward the space, and is the most variably positioned region in the C terminus (25). A similar helix-loop structure (548–557) exists in HSP90 with several hydrophobic residues $Met^{546}$, $Met^{550}$, $Ala^{551}$, $Leu^{553}$, $Phe^{554}$, and $Ala^{556}$ lining on the hydrophobic interface of Helix 2. A follow-up mutagenesis study identified that a sequence of ANMERIMKA within the helix 2 region is important in binding to unliganded glucocorticoid receptor, and protecting its hydrophobic groove in the ligand binding domain (26).

Based on the knowledge of HSP90 and the crystal structure of gp96, a similar helix-loop structure (652–678) of gp96 emerged as an attractive candidate as the CBD of gp96. The loop structure of the CBD is potentially more flexible compared with other regions of gp96, and more importantly, it protrudes out toward solvent, making it readily available for mediating client protein interactions. Further support for the identification of this loop as a critical part of the gp96 CBD comes from its hydrophobic character, whereby Met, Tyr, and Trp residues are exposed to solvent, a relatively rare occurrence that implies a potential role in forming protein-protein interactions.

We have presented definitive evidence that identifies a C terminus loop structure of gp96 (652–678) is a critical region of the client binding domain of gp96 in chaperoning both integrins and TLRs. While this work identifies the locus of client-gp96 interactions, it is likely that gp96 may utilize different chaperoning mechanisms to fold TLRs comparing with integrins. This is supported by our findings that integrins but not TLRs are dependent on the Met pairs in the CBD region, based on the following evidence: (i) M2A mutant is able to fully restore the surface expression of both TLR2 and TLR4 (Fig. 3, *A* and *B*), as well as the functional responsiveness to multiple ligands (supplemental Fig. S1). It also retains its ability to bind to a TLR-specific co-chaperone CNPY3 (supplemental Fig. S2). (ii) However, M2A mutant is significantly impaired in conferring surface expression of multiple integrins (Fig. 3). Strikingly, although single M658A mutant is even more efficient than wild type gp96 in facilitating TLR2 surface expression, its ability to restore $\alpha$L integrin expression is significantly compromised (Fig. 3). (iii) The defect of M2A mutant in facilitating surface expression of integrin correlates directly to its reduced ability to bind to $\alpha$L (Fig. 5). The different folding mechanisms of TLR and integrins is also highlighted by the fact that TLR folding is dependent on both the ATPase activity and ATP-binding property of gp96, while the folding of integrin is only dependent on ATP binding (9, 11). In this regard, several questions remain unanswered. It is unclear how the twisted V structure of gp96 is shifted to a "closed" catalytic dimer, which is the ATP hydrolytic conformation of HSP90. It is also unclear how this conformation of gp96 is regulated by the binding or hydrolysis of ATP or ADP. Finally, it remains to be determined whether clients or cochaperones play any role in the conformational change of gp96, and it is unknown if the folding of integrins requires an as yet unidentified co-chaperone.

We believe that the identification of a discrete client-binding region in gp96 represents a major advance in route toward developing a gp96-specific inhibitor. A recent study reported that a peptide sequence targeting part of the charged linker region of gp96 was able to inhibit endotoxic shock when administered *in vivo* (36). It is noteworthy that CBD-targeted peptide is able to significantly inhibit gp96-integrin interaction. We are pursuing a CBD-targeted strategy to generate gp96-specific inhibitors for the treatment of inflammation and other diseases.

*Acknowledgments—We thank the past and present students and postdoctoral fellows in our laboratory for insightful discussions. We are especially grateful to Drs. Adam Adler and Pramod Srivastava for invaluable input.*

## REFERENCES

1. Chen, B., Piel, W. H., Gui, L., Bruford, E., and Monteiro, A. (2005) The HSP90 family of genes in the human genome: insights into their divergence and evolution. *Genomics* **86,** 627–637
2. Lee, A. S., Bell, J., and Ting, J. (1984) Biochemical characterization of the 94- and 78-kilodalton glucose-regulated proteins in hamster fibroblasts. *J. Biol. Chem.* **259,** 4616–4621
3. Mazzarella, R. A., and Green, M. (1987) ERp99, an abundant, conserved glycoprotein of the endoplasmic reticulum, is homologous to the 90-kDa heat shock protein (hsp90) and the 94-kDa glucose-regulated protein (GRP94). *J. Biol. Chem.* **262,** 8875–8883
4. Koch, G., Smith, M., Macer, D., Webster, P., and Mortara, R. (1986) Endoplasmic reticulum contains a common, abundant calcium-binding glycoprotein, endoplasmin. *J. Cell Sci.* **86,** 217–232
5. Srivastava, P. K., DeLeo, A. B., and Old, L. J. (1986) Tumor rejection antigens of chemically induced sarcomas of inbred mice. *Proc. Natl. Acad. Sci. U.S.A.* **83,** 3407–3411
6. Li, Z., and Srivastava, P. K. (1993) Tumor rejection antigen gp96/grp94 is an ATPase: implications for protein folding and antigen presentation. *EMBO J.* **12,** 3143–3151
7. Yang, Y., and Li, Z. (2005) Roles of heat shock protein gp96 in the ER quality control: redundant or unique function? *Mol. Cells* **20,** 173–182
8. Christianson, J. C., Shaler, T. A., Tyler, R. E., and Kopito, R. R. (2008) OS-9 and GRP94 deliver mutant $\alpha$1-antitrypsin to the Hrd1-SEL1L ubiquitin ligase complex for ERAD. *Nat. Cell Biol.* **10,** 272–282
9. Randow, F., and Seed, B. (2001) Endoplasmic reticulum chaperone gp96 is required for innate immunity but not cell viability. *Nat. Cell Biol.* **3,** 891–896
10. Yang, Y., Liu, B., Dai, J., Srivastava, P. K., Zammit, D. J., Lefrançois, L., and Li, Z. (2007) Heat shock protein gp96 is a master chaperone for toll-like receptors and is important in the innate function of macrophages. *Immunity* **26,** 215–226

11. Liu, B., Yang, Y., Qiu, Z., Staron, M., Hong, F., Li, Y., Wu, S., Hao, B., Bona, R., Han, D., and Li, Z. (2010) Folding of Toll-like receptors by the HSP90 paralogue gp96 requires a substrate-specific cochaperone. *Nat. Commun.* **1,** 1–10
12. Liu, B., and Li, Z. (2008) Endoplasmic reticulum HSP90b1 (gp96, grp94) optimizes B-cell function via chaperoning integrin and TLR but not immunoglobulin. *Blood* **112,** 1223–1230
13. Luo, B., Lam, B. S., Lee, S. H., Wey, S., Zhou, H., Wang, M., Chen, S. Y., Adams, G. B., and Lee, A. S. (2011) The endoplasmic reticulum chaperone protein GRP94 is required for maintaining hematopoietic stem cell interactions with the adult bone marrow niche. *PLoS One* **6,** e20364
14. Staron, M., Wu, S., Hong, F., Stojanovic, A., Du, X., Bona, R., Liu, B., and Li, Z. (2011) Heat-shock protein gp96/grp94 is an essential chaperone for the platelet glycoprotein Ib-IX-V complex. *Blood* **117,** 7136–7144
15. Staron, M., Yang, Y., Liu, B., Li, J., Shen, Y., Zuñiga-Pflücker, J. C., Aguila, H. L., Goldschneider, I., and Li, Z. (2010) gp96, an endoplasmic reticulum master chaperone for integrins and Toll-like receptors, selectively regulates early T and B lymphopoiesis. *Blood* **115,** 2380–2390
16. Morales, C., Wu, S., Yang, Y., Hao, B., and Li, Z. (2009) *Drosophila* glycoprotein 93 Is an ortholog of mammalian heat shock protein gp96 (grp94, HSP90b1, HSPC4) and retains disulfide bond-independent chaperone function for TLRs and integrins. *J. Immunol.* **183,** 5121–5128
17. Medzhitov, R. (2007) Recognition of microorganisms and activation of the immune response. *Nature* **449,** 819–826
18. Jin, M. S., and Lee, J. O. (2008) Structures of the toll-like receptor family and its ligand complexes. *Immunity.* **29,** 182–191
19. Kawai, T., and Akira, S. (2007) TLR signaling. *Semin Immunol.* **19,** 24–32
20. Luo, B. H., Carman, C. V., and Springer, T. A. (2007) Structural basis of integrin regulation and signaling. *Annu. Rev. Immunol.* **25,** 619–647
21. Hynes, R. O. (2002) Integrins: bidirectional, allosteric signaling machines. *Cell* **110,** 673–687
22. Miranti, C. K., and Brugge, J. S. (2002) Sensing the environment: a historical perspective on integrin signal transduction. *Nat. Cell Biol.* **4,** E83–90
23. Ali, M. M., Roe, S. M., Vaughan, C. K., Meyer, P., Panaretou, B., Piper, P. W., Prodromou, C., and Pearl, L. H. (2006) Crystal structure of an Hsp90-nucleotide-p23/Sba1 closed chaperone complex. *Nature* **440,** 1013–1017
24. Dollins, D. E., Warren, J. J., Immormino, R. M., and Gewirth, D. T. (2007) Structures of GRP94-nucleotide complexes reveal mechanistic differences between the hsp90 chaperones. *Mol. Cell* **28,** 41–56
25. Harris, S. F., Shiau, A. K., and Agard, D. A. (2004) The crystal structure of the carboxy-terminal dimerization domain of htpG, the *Escherichia coli* Hsp90, reveals a potential substrate binding site. *Structure* **12,** 1087–1097
26. Fang, L., Ricketson, D., Getubig, L., and Darimont, B. (2006) Unliganded and hormone-bound glucocorticoid receptors interact with distinct hydrophobic sites in the Hsp90 C-terminal domain. *Proc. Natl. Acad. Sci. U.S.A.* **103,** 18487–18492
27. Liu, B., Yang, Y., Dai, J., Medzhitov, R., Freudenberg, M. A., Zhang, P. L., and Li, Z. (2006) TLR4 up-regulation at protein or gene level is pathogenic for lupus-like autoimmune disease. *J. Immunol.* **177,** 6880–6888
28. Pearl, L. H., and Prodromou, C. (2006) Structure and mechanism of the Hsp90 molecular chaperone machinery. *Annu. Rev. Biochem.* **75,** 271–294
29. Cadepond, F., Binart, N., Chambraud, B., Jibard, N., Schweizer-Groyer, G., Segard-Maurel, I., and Baulieu, E. E. (1993) Interaction of glucocorticosteroid receptor and wild-type or mutated 90-kDa heat shock protein coexpressed in baculovirus-infected Sf9 cells. *Proc. Natl. Acad. Sci. U.S.A.* **90,** 10434–10438
30. Sullivan, W. P., and Toft, D. O. (1993) Mutational analysis of hsp90 binding to the progesterone receptor. *J. Biol. Chem.* **268,** 20373–20379
31. Shaknovich, R., Shue, G., and Kohtz, D. S. (1992) Conformational activation of a basic helix-loop-helix protein (MyoD1) by the C-terminal region of murine HSP90 (HSP84). *Mol. Cell Biol.* **12,** 5059–5068
32. Meyer, P., Prodromou, C., Hu, B., Vaughan, C., Roe, S. M., Panaretou, B., Piper, P. W., and Pearl, L. H. (2003) Structural and functional analysis of the middle segment of hsp90: implications for ATP hydrolysis and client protein and cochaperone interactions. *Mol. Cell* **11,** 647–658
33. Sato, S., Fujita, N., and Tsuruo, T. (2000) Modulation of Akt kinase activity by binding to Hsp90. *Proc. Natl. Acad. Sci. U.S.A.* **97,** 10832–10837
34. Vaughan, C. K., Gohlke, U., Sobott, F., Good, V. M., Ali, M. M., Prodromou, C., Robinson, C. V., Saibil, H. R., and Pearl, L. H. (2006) Structure of an Hsp90-Cdc37-Cdk4 complex. *Mol. Cell* **23,** 697–707
35. Zhao, Q., Boschelli, F., Caplan, A. J., and Arndt, K. T. (2004) Identification of a conserved sequence motif that promotes Cdc37 and cyclin D1 binding to Cdk4. *J. Biol. Chem.* **279,** 12560–12564
36. Kliger, Y., Levy, O., Oren, A., Ashkenazy, H., Tiran, Z., Novik, A., Rosenberg, A., Amir, A., Wool, A., Toporik, A., Schreiber, E., Eshel, D., Levine, Z., Cohen, Y., Nold-Petry, C., Dinarello, C. A., and Borukhov, I. (2009) Peptides modulating conformational changes in secreted chaperones: from *in silico* design to preclinical proof of concept. *Proc. Natl. Acad. Sci. U.S.A.* **106,** 13797–13801